Pharmacogn J. 2025; 17(2): 121-128
A Multifaceted Journal in the field of Natural Products and Pharmacognosy
www.phcogj.com

Original Article

Myricitrin-Mediated Biogenic Silver Nanoparticle Synthesis, Characterization, and its Antioxidant, Anticancer, and DNA Cleavage Activities

Pallab Kar[1], Ayodeji O. Oriola[2,*], Moganavelli Singh[3], Adebola O. Oyedeji[1,2]

ABSTRACT

Introduction: Myricitrin (MY) is a potent antioxidant flavonoid that has recently gained research interest due to its wide applications in food, cosmetics, and medicine. **Objective:** The current work reports MY, its isolation and characterization from *Eugenia uniflora* leaves, and green synthesis with $AgNO_3$ to afford myricitrin-based silver nanoparticles (MY-Ag NPs). **Materials and Methods:** The biosynthesized nanoparticles (NPs) were characterized using UV, field emission scanning electron microscopy (FESEM), energy-dispersive X-ray spectroscopy (EDX), X-ray diffraction (XRD), High-resolution transmission electron microscopy (HRTEM) and Dynamic light scattering (DLS) methods. Antioxidant, anti-cancer, and DNA cleavage activities were based on standard *in vitro* bioassay methods. **Results:** The UV-vis absorption peak at 430 nm suggests the formation of silver-based NPs. The FESEM imaging showed spherical-to-cubical shaped MY-Ag NPs with an average size of 45.35 nm. The EDX analysis showed the presence of elemental Ag (89.40%) and N (10.22%), suggesting a successful synthesis. The XRD analysis revealed various peaks at 38.37^0, 43.56^0, 63.76^0, and 77.77^0, which suggest metallic silver reflections, further establishing the crystallinity of NPs. The MY-Ag NPs inhibited O_2^-, OH^-, H_2O_2, and NO free radicals in a dose-dependent manner. At 50 and 80 µg/mL, it demonstrated a better inhibitory effect on OH- radical than *L*-ascorbic acid. The cytotoxicity (IC_{50}) against human cancer cell lines of the kidney (ACHN) and the liver (HepG2) were 54.21 ± 0.06 µg/mL and 33.36 ± 2.25 µg/mL respectively at 48 h post-treatment. Lastly, at 20 mg/mL for 120 minutes, MY-Ag NPs cleaved DNA, acting as chemical nucleases. This may suggest its capacity to impede cancer cells by cleaving the genome. **Conclusion:** Therefore, this study has shown that Myricitrin-based Ag NPs possess notable antioxidant and cytotoxicity that can be further exploited in the search for newer anticancer agents.

Keywords: Myricitrin, Silver nanoparticles, Antioxidant, Anticancer, DNA cleavage.

Pallab Kar[1], Ayodeji O. Oriola[2,*], Moganavelli Singh[3], Adebola O. Oyedeji[1,2]

[1]*African Medicinal Flora and Fauna Research Niche Area, Walter Sisulu University Nelson Mandela Drive, P/Bag X1, Mthatha 5117, SOUTH AFRICA.*

[2]*Department of Chemical and Physical Sciences, Walter Sisulu University, Nelson Mandela Drive, P/Bag X1, Mthatha 5117, SOUTH AFRICA.*

[3]*Nano-Gene and Drug Delivery Group, Discipline of Biochemistry, University of KwaZulu-Natal, Private Bag, Durban X54001, SOUTH AFRICA.*

Correspondence

A.O. Oriola

Department of Chemical and Physical Sciences, Walter Sisulu University, Nelson Mandela Drive, P/Bag X1, Mthatha 5117, SOUTH AFRICA.

E-mail: aooriola@gmail.com

History

- Submission Date: 18-01-2025;
- Review completed: 22-02-2025;
- Accepted Date: 03-03-2025.

DOI : 10.5530/pj.2025.17.17

Article Available online

http://www.phcogj.com/v17/i2

INTRODUCTION

Nanotechnology is currently one of the materials science research fields with the highest activity. The past fifty years have been devoted to material scientists investigating the potential uses of nanoparticles (NPs).[1] The nanoparticles' distribution, form, and size can influence their improved or novel characteristics. Because they are smaller than macro-sized materials, nanoparticles have a larger surface area. Metal nanoparticles' inherent properties are primarily determined by their size, shape, composition, crystallinity, and morphology.[2] Due to their small size and novel characteristics, they have versatile uses in biological, medical, electrical, and chemical sciences.[3] Among the metal nanoparticles, AgNPs, or silver nanoparticles, are at least one dimension in size, with values between 1 and 100 nm. AgNPs have a wide range of biological characteristics and are a very versatile nanomaterial.[4] AgNPs have been shown to have antifungal, antibacterial, anti-inflammatory, and anticancer properties.[5,6] These days, the new method for producing green or biological nanoparticles is to use different bioactive substances, including plant extracts,[7,8] microorganisms,[9] and many other sources[10] instead of hazardous, poisonous chemicals. This approach is not only hopeful and environmentally benign, but it also lowers carbon emissions and encourages sustainable development.[11] Among these techniques, biomass, especially flavonoids, are said to be effective in converting Ag+ ions into AgNPs. Due to their abundant sources, excellent synthesis efficiency, and extensive biological activities and pharmacological effects,[12] flavonoids have significant practical value. Myricitrin (MY) is a naturally occurring dietary flavonoid commonly found in fruit, vegetables, tea, and herbal remedies.[13] Numerous biological activities are associated with MY, including antibacterial,[14] antiviral,[15] antioxidant,[16] anti-inflammatory, anticancer,[17] suppression of urease,[18] and more. Myricitrin is currently widely utilized in various industries, including food, cosmetics, pharmaceuticals, and medicine. The current work offers a novel approach to the isolation and characterization of myricitrin from *Eugenia uniflora* and the synthesis of environmentally friendly Agness to convert silver ions into nanoparticles without hazardous chemical additions. The characterization of the synthesized nanoparticles using UV, field emission scanning electron microscopy (FESEM), energy-dispersive X-ray spectroscopy (EDX), X-ray diffraction (XRD), High-resolution transmission electron microscopy (HRTEM) and Dynamic light scattering (DLS) analysis was conducted. Furthermore, the antioxidant, anti-cancer, and DNA cleavage activities of myricitrin-mediated AgNPs were studied.

Cite this article: Kar P, Oriola AO, Singh M, Oyedeji AO. Myricitrin-Mediated Biogenic Silver Nanoparticle Synthesis, Characterization, and its Antioxidant, Anticancer, and DNA Cleavage Activities. Pharmacogn J. 2025;17(2): 121-128.

MATERIALS AND METHODS

Plant material

The leaves of *Eugenia uniflora* were collected in March 2021 at Obafemi Awolowo University (O.A.U.), Ile-Ife, Nigeria (GPS coordinates: N 7˚3103.799200, E 4˚31034.852800). The collection was authenticated at the Ife Herbarium, O.A.U., Ile-Ife, with a voucher number IFE 16589. The leaves separated from their branches and air-dried away from direct sunlight inside the screen house with frequent turning. The dried leaves were powdered and kept in an airtight plastic bag for further use.

Isolation of Myricitrin

The method of Oriola *et al.*[19] was followed. 1 kg of the leaf powder was extracted with 5 L of EtOH/H_20 (4:1) at 60 ˚C under reflux for 4 h. It was filtered after cooling and concentrated to dryness *in vacuo* using a Heidolph 110 Laborata rotavapor (Heidolph Instruments GmbH & Co. KG, Schwabach, Germany). The afforded extract (110 g) was suspended in 400 mL of distilled water and successively partitioned with n-hexane (Hex) (2 × 500 mL), dichloromethane (DCM, 3 × 500 mL), and ethyl acetate (EtOAc, 4 × 500 mL). The EtOAc fraction (15 g) was adsorbed unto 30 g silica gel and eluted on a 160 g silica gel column. The gradient elution process was followed with increasing polarity from Hex (100%), through Hex-EtOAc (9:1, 8:2, 6:4, 4:6, 2:8), to EtOAc-MeOH (95:5, 9:1, 8:2, 7:3, 5:5 and 3:7). A total fifty-one eluates were collected in 500 mL flasks. They were pooled into five subfractions **Fr. 1–5** based on TLC analysis. Subfraction Fr 4 was further fractionated on the Sephadex LH-20 column by isocratic elution with DCM-MeOH (7:3), affording **Fr. 4a–d**. Subfraction **Fr. 4b** gave a yellowish amorphous solid (39 mg), with a single yellow spot (R_f 0.49) which later charred after spraying with 10% sulfuric acid and heated at 105^{O}C. The subfraction gave a melting point range of 197–198 ˚C, confirming it to be a pure compound.

Spectroscopic and Spectrometric Analyses

The isolated compound was analyzed on the Avance 600 MHz Spectrometer (Bruker Biospin GmbH-Rheinstetten, Germany) and the Quadrupole Time-of-Flight (QToF) Synapt G2 Mass Spectrometer (Waters Corporation, Milford, MA, USA) both situated at the Central Analytical Facility, Stellenbosch University, South Africa. The isolated compounds' 1D- and 2D NMR spectral data were acquired in DMSO-d_6 (Sigma-Aldrich Chemie GmbH, Taufkirchen, Germany). Tetramethyl silane was the internal standard, while chemical shift values (δ) were recorded from 0-14 ppm and 0-220 ppm on the 1H and the 13C NMR spectra, respectively. The mass determination was achieved via electrospray ionization method (HRESI-MS). The molecular weight of the isolated compound was read in the positive ion mode on the mass spectrometer in mass-to-charge ratio (*m/z*), over a scan range of *m/z* 100–1000.

Synthesis of nanoparticle from silver nitrate ($AgNO_3$) using myricitrin

Myricitrin silver nanoparticles (MY-Ag NPs) were synthesized by combining $AgNO_3$ [1.575 g (0.103 M) diluted in 90 mL of distilled water] with myricitrin (30 mg dissolved in 10 mL of distilled water). The solution turned from colourless to greyish brown after boiling it at 80 °C for 6 to 8 hours while being stirred magnetically. After that, the solution was centrifuged for 20 minutes at room temperature at 6000 rpm. The samples were stored at 4 °C after air drying.[5,20,21]

Characterization of silver nanoparticle

MY-Ag NPs were characterized by UV, FESEM, EDX, HRTEM, XRD, and DLS analyses. Biogenically generated nanoparticles were characterized using UV-visible spectroscopy, and a graph was also plotted. The powdered MY-Ag NPs were placed on copper mesh for FESEM and EDX investigation, and a gold sputtering apparatus applied a 3 nm gold covering. FESEM (German manufacturer Carl Zeiss; model: SIGMA-0261) was used to record the AgNPs' surface morphology at a 3 kV accelerating voltage at 20,000 × magnifications. A High-resolution Transmission Electron Microscope (Model name FEI TECNAI G2 F300) operating at 300KV was used to examine the size and morphology of biogenically produced MY-Ag NPs. The carbon-coated copper stub was covered with a tiny drop of nanoparticle suspension, which was then exposed to HR-TEM after air drying. The crystal structure of MY-Ag NPs was obtained using high-resolution XRD (Panalytical Emperian diffractometer, Netherland, 40 mA, 40 kV, λ=1.54056 Å). Differential light scattering (DLS) experiments were performed to ascertain the size distribution, stability, and zeta potential of biogenically produced MY-Ag NPs. A DLS analyzer (Model: NANO ZS, Manufacturer: Malvern Analytical Ltd.) was used for these analyses. Water with a count rate of 152.6 Kcps and a temperature of 25 °C was utilized as the dispersion medium in this experiment.[5]

Determination of *in-vitro* antioxidant activity

Nitric oxide (NO) radical scavenging assay

The quantification technique of the Griess-Ilosvoy reaction at physiological pH[22] was used to measure the nitric oxide radical scavenging activity with minor adjustments. Briefly, phosphate-buffered saline (pH 7.4), sodium nitroprusside (SNP; 10 mM), and different concentrations of silver nitrate (SN), myricitrin, and MY-Ag NPs (0-200µg/mL) were mixed and made the final volume of 3 mL. After the mixture was thoroughly vortexed and incubated for 150 minutes at 25 °C, 0.5 mL of the pre-incubated reaction mixture was mixed with 1 mL of sulfanilamide (0.33%), which was diluted in 20% glacial acetic acid and allowed to sit at room temperature for 5 minutes. To facilitate colour production, 1 mL of N-(1 -Naphthyl) ethylenediamine dihydrochloride (NEED; 0.1%) was added, and the mixture was kept at 25 °C for 30 minutes. The absorbance was measured at 540 nm using distilled water as a blank. Curcumin functioned as a standard reference. The percent of inhibition was calculated according to the following equation I:

The equation I: Percentage of scavenging= $\frac{A0-A1}{A0} \times 100$

Where A_0= absorbance of the control and A_1= absorbance in the presence of samples and standard.

Hydrogen peroxide scavenging assay

The hydrogen peroxide (H_2O_2) scavenging capacity was calculated using a modified version of Long *et al.*[23]. H_2O_2 (50 mM) and different concentrations of silver nitrate (SN), myricitrin, and MY-Ag NPs (0-200 µg/mL) were combined in a screw-capped bottle, and the mixture was allowed to dark-incubate for 30 minutes at room temperature (≈25 °C). Next, 90 µL of H_2O_2, 10 µL of HPLC-grade methanol, and 0.9 ml of FOX reagent (made by combining 9 volumes of 4.4 mM BHT in HPLC-grade methanol with 1 volume of 1 mM xylenol orange and 2.56 mM ammonium ferrous sulfate in 0.25 M H_2SO_4) were added. After giving the mixture a gentle vortex and letting it sit for 30 minutes, the absorbance at 560 nm was determined. Ascorbic acid was utilized as a positive control. The percentage inhibition was calculated as before using equation I.

Hydroxyl radical scavenging assay

Hydroxyl radical scavenging activity was conducted using the Fenton reaction model[24] with a small modification. 2-deoxy-2-ribose (2.8 mM), monopotassium phosphate-potassium hydroxide buffer (KH_2PO_4-KOH; 20 mM; pH 7.4), $FeCl_3$ (100 µM), ethylene diamine tetra acetic acid (EDTA; 100 µM), hydrogen peroxide (H_2O_2; 1.0 mM), ascorbic acid (100 µM), and varying concentrations of silver nitrate (SN), myricitrin,

and MY-Ag NPs (0–200µg/mL) were added to the reaction mixture until a final volume of 1 mL was achieved. After carefully mixing the reaction mixture, it was incubated for 60 minutes at 37 °C. Following the incubation period, the 0.5 ml mixture was carefully transferred into a fresh tube and mixed with 1 mL each of aqueous thiobarbituric acid (TBA; 1%) and TCA (2.8%). Once more, the finished mixture was incubated for 15 minutes at 90 °C. The absorbance at 532 nm was measured after the mixture had cooled to room temperature compared to an appropriate blank solution. A positive control was employed, such as ascorbic acid. The percentage inhibition was calculated as before using equation I.

Superoxide radical scavenging assay

The assay was conducted following Fontana *et al.*[25]. The nitro-blue tetrazolium (NBT) is reduced to purple formazan in the presence of the nonenzymatic PMS/NADH system, which produces superoxide radicals when exposed to oxygen. Phosphate buffer (20 mM, pH 7.4), NBT (50 µM), PMS (15 µM), NADH (73 µM), and varying doses (0-200 µg/mL) of silver nitrate (SN), myricitrin, and MY-Ag NPs were combined to create a reaction mixture (1 ml). After gently vortexing the mixtures, they were incubated for five minutes at room temperature. The amount of formazan produced was estimated by measuring the absorbance at 562 nm compared to the equivalent blank samples. Quercetin served as a positive reference. The percentage inhibition was calculated as before using equation I.

In-vitro anti-cancer activity

Cell culture

The South African company Highveld Biologicals (Pty) Ltd., located in Lyndhurst, provided the Vero, ACHN, and HepG2 cell lines. The cells were maintained using Dulbecco's Modified Eagle Medium/Nutrient Mixture F-12 Ham (DMEM/F12). 10% fetal bovine serum (FBS), 100 mg/ml streptomycin, 100 units/ml penicillin, 0.14% sodium bicarbonate, and 0.1 mM sodium pyruvate were added as supplements. For a duration of 24 hours, cells were cultured on 35 mm petri dishes at 37 °C, 5% CO_2, and 95% humidity in a CO_2 incubator.

MTT assay

A standard MTT test was used to assess cell viability, following Denizot and Lang's[26] instructions. The effects of different doses of myricitrin, and MY-Ag NPs on the inhibition of cancer cell proliferation were examined using the Vero normal cell line, ACHN human renal adenocarcinoma cell line, and Hep G2 human liver cancer cell line. The cells were grown to confluence in a DMEM complete medium enhanced with 10% FBS and 1% penicillin-streptomycin solution. The medium was kept at 37 °C in an incubator with 5% CO_2 humidity and a humidified environment. Trypsinized and counted exponentially developing cultured cells were sown at 2×104 cells/well density in a 96-well plate. The cells were treated with escalating doses of myricitrin and MY-Ag NPs (40, 80, 120, 160, 200 µg/mL) as well as negative control (water) and positive control 5-Fluorouracil (50 µM) for 48 hours following a 24-hour period of adherence. Following the above-mentioned incubation conditions, 10 µL of MTT solution (5 mg/mL) was applied to each well, and the wells were left in the dark for three hours. After the medium was carefully removed, 50 µL of isopropanol was used to dissolve the formazan that had developed in the wells, and the plates were left on a plate shaker for five minutes. The absorbance was determined at 595 nm with an iMarkTM Microplate Absorbance Reader (Bio-Rad, USA). Every experiment was run via four duplicates.

DNA cleavage assay

Agarose gel electrophoresis was used to examine the DNA cleavage capacity of MY-Ag NPs.[27,28] The target DNA molecules were plasmid DNA (pBR322). For two hours at 37 °C, 20 µL MY-Ag NPs at 10 mg/mL and 20 mg/mL with 3 µL plasmid DNA were reacted. Following incubation, each tube was filled with 2 µL of loading buffer (pH 7.0), which contained 25% bromophenol blue, 30% glycerol, and 0.25% xylene cyanol. Afterward, each sample solution was loaded onto a 1% (w/v) agarose gel that contained 0.5µg/mL of ethidium bromide. A double digest of lambda DNA/EcoRI/HindIII (2µL) was loaded as a molecular marker to ascertain the molecular size of the nearby genomic DNA. Using a mini-submarine gel electrophoresis equipment and an electrophoresis power supply unit, the electrophoresis was performed for 2 hours at 50 Volt in 0.5X TBE buffer (Tris-Borate-EDTA). Once the gel had undergone electrophoresis, it was photographed and observed under a UV transilluminator.

Statistical analysis

To compare the activity of MY-Ag NPs and references, Student's t-Test integrated with the KyPlot program (version 5.0) was used for statistical analysis.

RESULTS AND DISCUSSION

Characterization of isolated compound

Myricitrin*:* Yellow amorphous solid, m.p. 197–198°C. **HR-ESI–MS** (m/z, % rel. int.): *m/z* 465.1033 ($C_{21}H_{20}O_{12}$), found *m/z* 465.1022 $[M+H]^+$ (100%); *m/z* 319.0454 ($C_{15}H_{11}O_8$), found 319.0441 [M–Rhamnosyl]$^+$ (89%) (Figure S1); **^{1}H NMR** (600 MHz, DMSO-d_6) δ 0.85 (3H, *d*, *J* = 6.1 Hz, H-6''), 3.15 (1H, *t*, *J* = 9.3 Hz, H-4''), 3.36 (1H, *dq*, *J* = 5.1, 6.5 Hz, H-5''), 3.56 (1H, *dd*, *J* = 2.5, 4.5 Hz, H-3''), 3.98 (1H, *d*, *J* = 3.3 Hz, H-2''), 5.20 (1H, *s*, H-1''), 6.20 (1H, *d*, *J* = 2.5 Hz, H-6), 6.37 (1H, *d*, *J* = 2.5 Hz, H-8), 6.91 (2H, *d*, *J* = 6.9 Hz, H-2', H-6'); **^{13}C NMR** (150 MHz, DMSO-d_6): δ 157.5 (C-2), 134.3 (C-3), 177.8 (C-4), 104.1 (C-4a), 161.4 (C-5), 98.7 (C-6), 164.2 (C-7), 93.6 (C-8), 156.5 (C-8a), 119.6 (C-1'), 107.9 (C-2'/6'), 145.8 (C-3'/5'), 136.5 (C-4'), *L*-Rhamnose: 101.9 (C-1''), 70.0 (C-2''), 70.4 (C-3''), 71.3 (C-4''), 70.6 (C-5''), 17.5 (C-6'') (Figure S2).

Structure elucidation of isolated compound

The ^{1}H NMR spectrum showed three aromatic protons δ_H 6.20, 6.37 and two chemically equivalent protons at δ_H 6.91, and the most deshielded signals at δ_H 12.68, suggesting a flavonoid core. The presence of one rhamnose sugar unit was revealed by six proton resonances at δ_H 5.21 – 0.85. The hump singlet signal at δ_H 12.68 ppm is an indication of an intermolecular hydrogen bond between the proton of the hydroxyl signal (5-OH) with the oxygen of the neighbouring carbonyl at position C-4, which suggests it to be a flavonol glycoside. The ^{13}C NMR showed twenty-one signals, suggesting a C_{21} compound. The most deshielded signal at δ_C 177.8 indicates the presence of a carbonyl functional group of an enone, which is typical of the C=O at position C-4 of flavonoid. The HSQC spectrum showed the rhamnose carbon signals with the anomeric carbon (C-1'') resonating at δ_C 101.9, and the C-2 to C-5 signals at δ_C 70.0–71.3. In the HMBC spectrum, a long-range coupling ($^3J_{CH}$) was observed between the methyl proton at δ_H 0.85 and a sugar carbon at δ_C 71.3, confirming the sugar to be a Rhamnose. Additionally, the O-Rhamnosyl linkage was confirmed in the HMBC experiment, with a long-range coupling between the anomeric proton (H-1'') at δ_H 5.17 and the C-3 at δ_C134.3. The acquired NMR spectral data agreed with that of Myricetin-3-O-rhamnoside, a flavonol glycoside reported by Kassem *et al.*[29] and Oriola *et al.*[19]. The HR-ESI-MS data agreed with the NMR elucidated Myricetin-3-O-rhamnoside structure. The mass fragmentation pattern showed a quasi-molecular ion $[M+H]^+$ peak at *m/z* 465.1022, consistent with the molecular formula $C_{21}H_{20}O_{12}$ for Myricitrin. The daughter ion at *m/z* 319.0441 indicates a homolytic cleavage of rhamnosyl ion $[M-146]^+$, affording the Myricetin flavonoid core.

Characterization of biogenic silver nanoparticles (AgNPs)

The production of MY-Ag NPs in the solution is confirmed by UV-Vis spectroscopy, which displays characteristic peaks for MY-Ag NPs at 430 nm (Figure 1A). According to Banerjee *et al.*[5], the synthesis of nanoparticles is confirmed by surface Plasmon resonances (SPR) spectra within the 400–500 nm wavelength range. MY-Ag NPs that have been biosynthesized had a spherical to cubical shape, as shown by the FESEM imaging (Figure 1B), which predominantly determined the size and surface morphology of the particles. According to our research, most MY-Ag NPs are ultrafine particles with a size of less than 100 nm. According to Das *et al.*[30], there are instances where the bulking of nanoparticles can occur because of solvent evaporating or crosslinking during sample preparation. The conversion of metallic silver into elemental silver was verified by EDX analysis (Figure 1C), demonstrating the presence of elemental Ag (89.40%). Despite multiple elements, including N (10.22%) and P (0.37%), only a significant, acute curve at~3 Kev was found in the EDX analysis; this is typical of biosynthesized MY-Ag NPs.[31] Based on HRTEM investigation, the majority of the biogenically produced MY-Ag NPs had a spherical shape and ranged in size from 10 to 50 nm. The well-dispersed and minimally accumulated nanoparticles were also observed in Figure 1D. According to earlier studies, nanoparticles' size and bioactivity are inversely related. Our research confirms MY-Ag NPs' compact size and high level of bioactivity.[30] This sample's X-ray diffraction (XRD) analysis reveals various peaks at 38.37°, 43.56°, 63.76°, and 77.77°. These peaks are indicative of metallic silver reflections, specifically (111), (200), (220), and (311). Previous findings support the crystalline nature of AgNPs and a sharp peak at 38.12° [reflection index (111)] can be identified by comparing its values with those given by the Joint Committee on Powder Diffraction Standards (JCPDS pdf no: 89-3722). Based on Bragg's law and a comparison of this data with the Debye-Scherrer formula, the average size of the nanoparticle is 45.35 nm (Figure 1E).[31] The size distribution of the produced MY-Ag NPs, according to DLS analysis (Figure 1F), ranges from 1 nm to 80 nm, and the average size of MY-Ag NPs is 45nm.

Determination of *in-vitro* antioxidant activity

Biological macromolecules, such as DNA and proteins, are harmed by superoxide anions ($O_2^{\cdot-}$) produced during different metabolic reactions. Singlet oxygen radicals and hydroxyl radicals, which are harmful, are two forms of radicals that the superoxide anion itself can produce. Figure 2A shows that the My-Ag NPs produced through biogenesis have a significant capacity to scavenge superoxide (69.26 ±

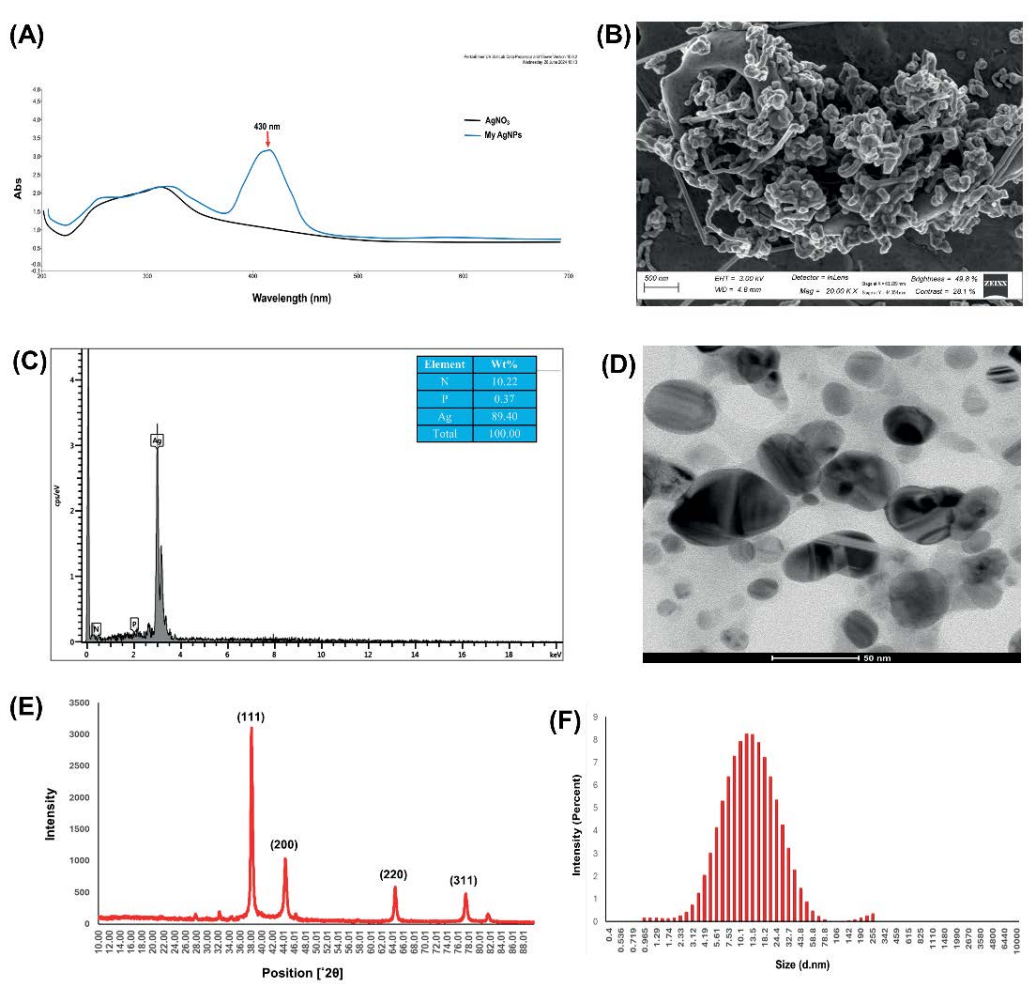

Figure 1: Characterization of biogenically synthesized silver nanoparticles (AgNPs): **(A)** UV Spectroscopy showing characteristics peaks at 430 nm. **(B)** Field emission Scanning electron microscopy (FE-SEM) image of My-Ag NPs. **(C)** EDX mapping and elemental profile of biosynthesized My-Ag NPs. **(D)** HR-TEM analysis of My-Ag NPs. **(E)** XRD pattern of biosynthesized biosynthesized My-Ag NPs. **(F)** Dynamic light scattering (DLS) analysis shows the size distribution pattern of My-Ag NPs.

1.36 % at 200 µg/ml) compared to SN (silver nitrate) and the compound myricitrin. According to Banerjee *et al.*[6], the neutralization of hydroxyl radicals by My-Ag NPs (75.43 ± 0.60 % at 200 µg/ml) safeguards cells and contributes to forming a stable cellular environment (Figure 2B). Although nitric oxide is a crucial signalling molecule, excess can function as reactive oxygen species (ROS) and harm tissues and cells. MY-Ag NPs exhibited nitric oxide scavenging activity (54.37 ± 1.90 % at 200 µg/ml) that responded in a dose-dependent manner compared to SN (silver nitrate) and the compound myricitrin. Nitric oxide and silver nanoparticles interact in living things to stop excessive nitric oxide buildup that could harm membranes (Figure 2C). In peroxisomes, superoxide anion and superoxide dismutase (SOD) combine to generate hydrogen peroxide (H_2O_2). As H_2O_2 builds up in cells, it reacts with other transition metals, such as Fe^{2+}, Cu^{2+}, etc. to form hydroxyl radical ($OH^{\cdot}$), which can damage DNA and cause lipid peroxidation.[32] MY-Ag NPs demonstrated a noteworthy H_2O_2 scavenging activity (69.26 ± 1.36 % at 200 µg/ml) in comparison to ascorbic acid as a reference (Figure 2D).[31] Accordingly, current research suggests that MY-Ag NPs may play a key role in the recovery of illnesses linked to oxidative stress.

In-vitro anti-cancer activity

The MTT test measured the cytotoxicity of the nanoparticles synthesized through the green route against the Vero, ACHN, and HepG2 cell lines. The three cell lines used in this study, Vero, ACHN, and HepG2, received similar quantities of the suspension medium and different dosages of MY-Ag NPs. It is important to note that the MY-Ag NPs and compound myricitrin appeared to be non-cytotoxic to the Vero cell line having demonstrated 76.95 ± 1.14 % and 73.95 ± 0.28 % viability at a concentration of 200 µg/ml with IC_{50} values of 261.08 ± 5.59 and 239.77 ± 4.58 µg/mL which reveals the probable safety of the MY-Ag NPs and the compound myricitrin (Figure 3A). The MY-Ag NPs exhibited substantial dose-dependent anticancer activity against the ACHN and HepG2 cell line with 31.32 ± 1.56 % and 34.71 ± 3.14 % viability at a concentration of 200 µg/mL (Figures 3B, C), with IC_{50} values of 54.21 ± 0.06 µg/mL, and 33.36 ± 2.25 µg/mL when compared to the compound myricitrin with IC_{50} values of 91.71 ± 2.23 µg/mL, and 116.45 ± 5.90 µg/mL after 48 hours of treatment. Additionally, 5-Fluorouracil (50 µM) was used as a positive control for ACHN and HepG2, exhibiting about 50% cell viability with IC_{50} values of 3.04 ± 0.07 µg/mL and 2.68 ± 0.04 µg/mL, respectively. The antiproliferative characteristics of the nanoparticles varied significantly across the tested normal and cancer cell lines. This suggests an intriguing variance in the target areas that the nanoparticles may use, indicated in the text to cause cytotoxicity in the tested cells. It is important to emphasize. Nevertheless, cytotoxicity alone does not qualify any medicinal material as a possible drug or chemical that can be drugged. Up until recently, it was unknown how these more modern therapeutic agents, including metal nanoparticles and their concentrations on normal cells, could have negative impacts on biological processes both *in vitro* and *in vivo*. Furthermore, it became necessary to respond to such adverse effects following the standards set for public health and safety in light of emerging public complaints in this field of study.[33] Overall, the current results provided experimental evidence that normal cells exposed

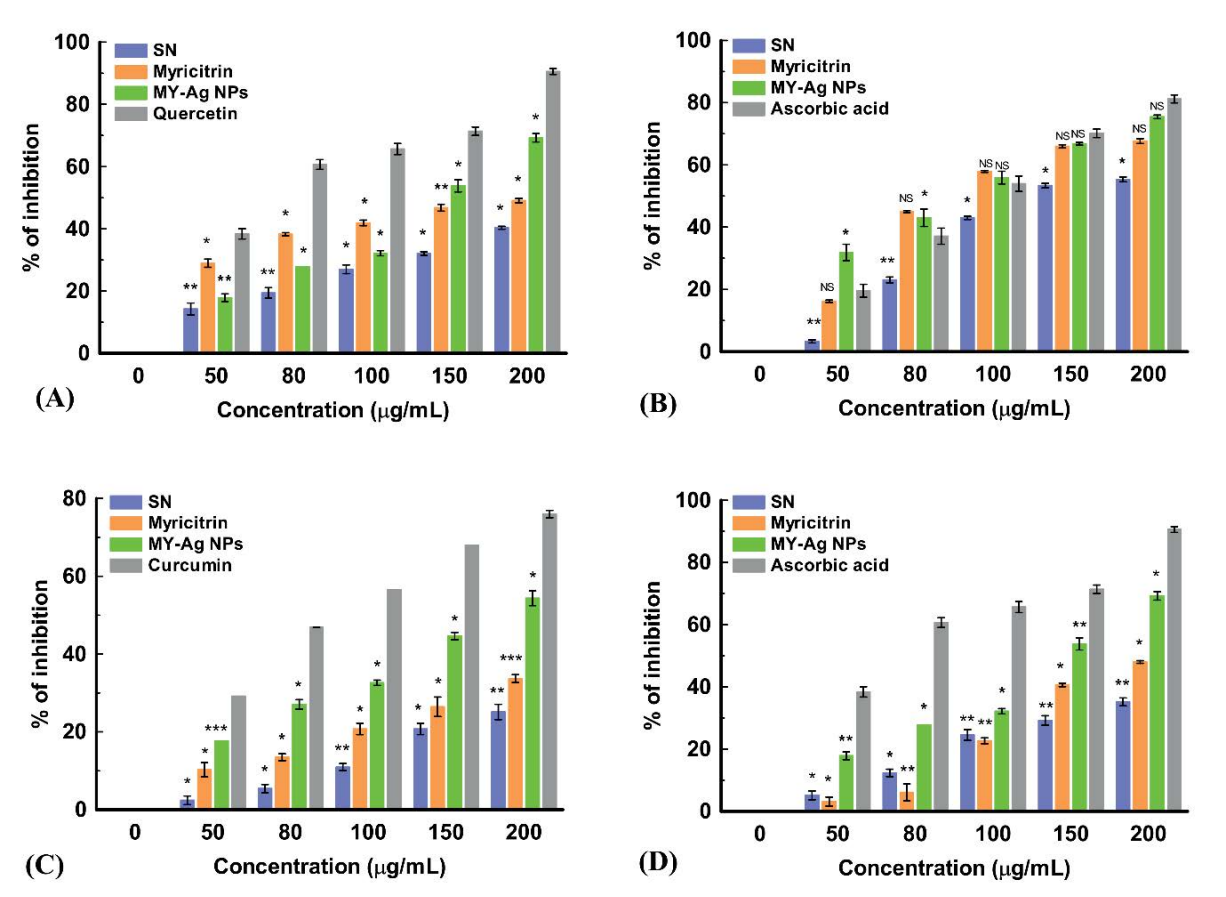

Figure 2: Antioxidant activity of synthesized silver nanoparticle **(A)** Superoxide radical. **(B)** Hydroxyl radical. **(C)** Nitric oxide. **(D)** Hydrogen peroxide scavenging activity. [Data expressed as mean ± S.D. *p<0.05; **p<0.01; ***p<0.001; NS- Non-significant when compared with standard].

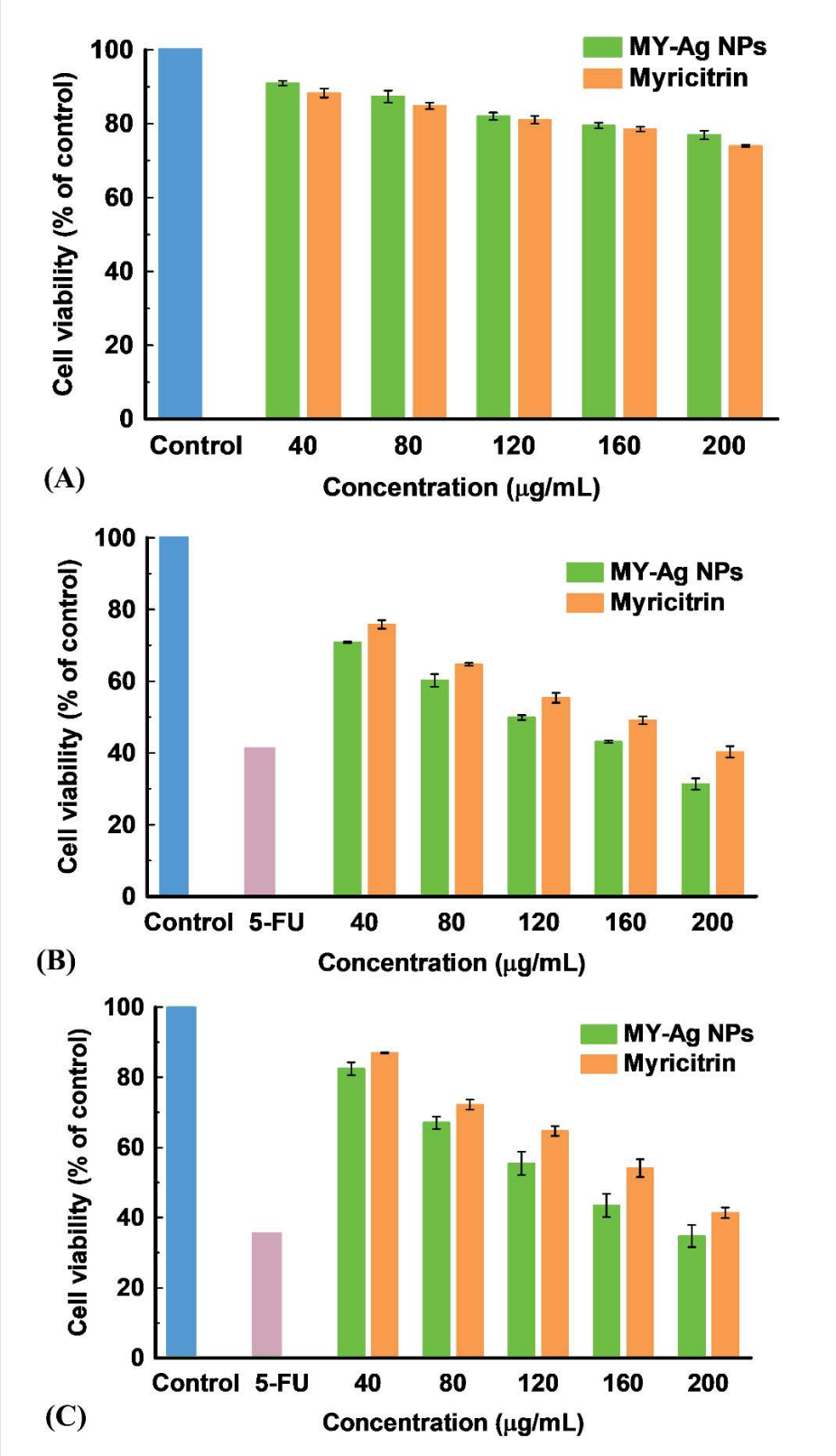

Figure 3: Cell viability (%) of **(A)** Vero normal cell line. **(B)** ACHN. **(C)** HepG2 cell line upon the exposure of various concentrations of silver nanoparticles (My-Ag NPs) for 48 h. [Data expressed as mean ± S.D.]

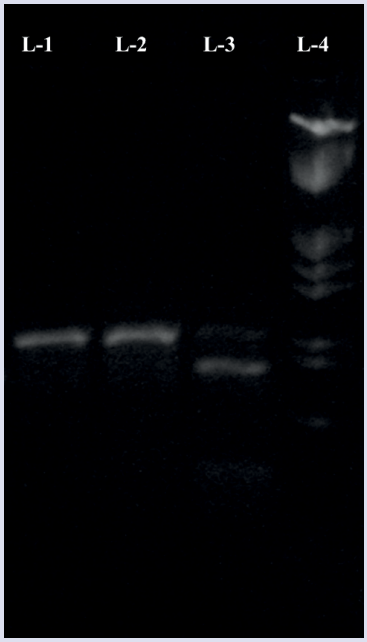

Figure 4: DNA cleavage activity of My-Ag NPs. **Lane 1**, pBR 322 DNA; **Lane 2**, pBR 322 DNA + 10 mg/mL of My-Ag NPs (120 mins incubation); **Lane 3,** pBR 322 DNA + 20 mg/mL of MY-Ag NPs (120 mins incubation); **Lane 4**, λ-DNA/EcoRI/HindIII double digest DNA ladder.

to the same dose of nanoparticles as cancer cell lines did not exhibit significant cytotoxic effects. This finding aligns with earlier research on biosynthesized AgNPs utilizing plant materials, including *Annona squamosa* leaf extract against the breast cancer MCF-7 cell line,[34] *Elaeagnus pyriformis* fruit extract against ACHN cancer cell lines,[5] and *Baccaurea ramiflora* against MDA-MB-231 and MCF7 cell lines.[6]

DNA cleavage assay

Gel electrophoresis was used to carry out the cleavage activity. Its effective DNA cleavage ability explains why the green-produced MY-Ag NPs cleave more effectively than the control.[35,36] AgNPs' interaction with plasmid DNA molecules was abundantly evident by the electrophoresis. When comparing Lanes 3 to control DNA (Lane1), Figure 4 illustrates how the bands differ. The findings demonstrated that, at a concentration of 20 mg/mL for 120 minutes, green-produced MY-Ag NPs cleaved DNA, acting as chemical nucleases. Observing the green production of MY-Ag NPs to cleave DNA suggests that newly synthesized green MY-Ag NPs impede cancer cell and pathogenic organism growth by cleaving the genome. Toxicological consequences of green-produced MY-Ag NPs require additional *in-vitro* and *in-vivo* investigations.

CONCLUSION

Phytochemical investigation of *E. uniflora* leaves led to the isolation and characterization of myricitrin (MY). MY-Ag NPs were successfully formed following green synthesis and characterization processes. The nanoparticles were spherical-to-cubical in shape, with an average size of 45.35 nm. It inhibited OH^- radicals considerably while significantly reducing ACHN and HepG2 cancer cell viability and acting as chemical nucleases. This may suggest the capacity of MY-Ag NPs to impede cancer cells by cleaving the genome. Therefore, this study has shown Myricitrin-based Ag NPs' biological potential as a candidate antioxidant and anticancer agent.

ACKNOWLEDGMENTS

The authors thank the Research Directorates of Walter Sisulu University (African Medicinal Flora and Fauna Niche Area and PDRFs) and NRF-Rated Researcher Incentive for their financial support.

CONFLICTS OF INTEREST

The authors declare that there is no conflict of interest.

SUPPORTING INFORMATION

Figure S1: HRESI-MS of Myricitrin; **Figure S2:** 1D and 2D NMR Spectra of Myricitrin.

REFERENCES

1. Gaur M, Misra C, Yadav AB, Swaroop S, Maolmhuaidh F, Bechelany M, Barhoum A Biomedical Applications of Carbon Nanomaterials: Fullerenes Quantum Dots Nanotubes Nanofibers and Graphene. Materials 2021; 14: 5978.
2. Barhoum A, Pal K, Rahier H, Uludag H, Kim IS, Bechelany M. Nanofibers as new-generation materials: From spinning and nano-spinning fabrication techniques to emerging applications. Appl Mater Today. 2019; 17: 1–35.
3. Kuppusamy P, Yusoff MM, Maniam GP, Govindan N. Biosynthesis of metallic nanoparticles using plant derivatives and their new avenues in pharmacological applications - An updated report. Saudi Pharmaceut J. 2016; 24: 473–484.
4. Durán N, Durán M, de Jesus MB, Fávaro WJ, Nakazato G, Nakazato G. Silver nanoparticles: A new view on mechanistic aspects on antimicrobial activity. Nanomed Nanotechnol Biol Med. 2016; 12: 789–799.
5. Banerjee S, Kar P, Sarkar I, Chhetri A, Mishra DK, Dutta A, Kumar A, Sinha B, Sen A. Structural elucidation and chemical characterization of underutilized fruit silverberry (*Elaeagnus pyriformis*) silver nanoparticles playing a dual role as anti-cancer agent by promoting apoptosis and inhibiting ABC transporters. S Afr J Bot. 2022; 145: 243-257.
6. Banerjee S, Islam S, Chattopadhyay A, Sen A, Kar P. Synthesis of silver nanoparticles using underutilized fruit *Baccaurea ramiflora* (Latka) juice and its biological and cytotoxic efficacy against MCF-7 and MDA-MB 231 cancer cell lines. S Afr J Bot. 2022; 145: 228-235.
7. Ahmed S, Ahmad M, Swami B L, Ikram S. A review on plants extract mediated synthesis of silver nanoparticles for antimicrobial applications: A green expertise. J Adv Res. 2016; 7: 17–28.
8. Zhang Y, Cheng X, Zhang Y, Xue X, Fu Y. Biosynthesis of silver nanoparticles at room temperature using aqueous aloe leaf extract and antibacterial properties. Colloids Surf A. 2013; 423: 63–68.
9. Park TJ, Lee KG, Lee SY. Advances in microbial biosynthesis of metal nanoparticles. Appl Microbiol Biotechnol. 2016; 100: 521–534.
10. Yuan CG, Huo C, Yu S, Gui B. Biosynthesis of gold nanoparticles using *Capsicum annuum* var *grossum* pulp extract and its catalytic activity. Phys E. 2017; 85: 19–26.
11. Gupta D, Thakur A, Gupta TK. Green and sustainable synthesis of nanomaterials: Recent advancements and limitations. Environ Res. 2023; 231: 116316.
12. Ong KC, Khoo HE. Biological effects of myricetin. General Pharmacology: The Vascular System. 1997; 29: 121–126.
13. Yao Y, Lin G, Xie Y, Ma P, Li G, Meng Q, Wu T. Preformulation studies of myricetin: a natural antioxidant flavonoid. Pharmazie. 2014; 69: 19–26.

14. Wang H, Du YJ, Song HC. α-Glucosidase and α-amylase inhibitory activities of guava leaves. Food Chem. 2010; 123: 6–13.
15. Tang X, Zhang C, Chen M, Xue Y, Liu T, Xue W. Synthesis and antiviral activity of novel myricetin derivatives containing ferulic acid amide scaffolds. New J Chem. 2020; 44: 2374–2379.
16. Zhang C, Zhang G, Liao Y, Gong D. Myricetin inhibits the generation of superoxide anion by reduced form of xanthine oxidase. Food Chem. 2017; 221: 1569–1577.
17. Ha TK, Jung I, Kim ME, Bae SK, Lee JS. Anti-cancer activity of myricetin against human papillary thyroid cancer cells involves mitochondrial dysfunction-mediated apoptosis. Biomed Pharmacother. 2017; 91: 378–384.
18. Trung HT, Huynh H TT, Thuy LNT, Minh HNV, Nguyen MN, Thi MNL. Growth-inhibiting bactericidal antibiofilm and urease inhibitory activities of *Hibiscus rosa sinensis* l Flower constituents toward antibiotic sensitive- and resistant-strains of *Helicobacter pylori*. ACS Omega. 2020; 5: 20080–20089.
19. Oriola AO, Miya GM, Singh M, Oyedeji AO. Flavonol glycosides from *Eugenia uniflora* leaves and their *in vitro* cytotoxicity antioxidant and anti-inflammatory activities. Sci Pharm. 2023; 91: 42.
20. Kar P, Banerjee S, Chhetri A, Sen A. Synthesis physicochemical characterization and biological activity of synthesized Silver and Rajat Bhasma nanoparticles using *Clerodendrum inerme*. J Phytol. 2021; 1: 64-71.
21. Kar P, Banerjee S, Saleh-E-In MM, Anandraj A, Kormuth E, Pillay S, Al-Ghamdi AA, Ali MA, Lee J, Sen A, Naidoo D Roy A, Choi YE. β-sitosterol conjugated silver nanoparticle-mediated amelioration of CCl_4-induced liver injury in Swiss albino mice. J King Saud Univ Sci. 2022; 34: 102113.
22. Garratt DC. The Quantitative Analysis of Drugs. Chapman and Hall Ltd Springer Japan 1964.
23. Long LH, Evans PJ, Halliwell B. Hydrogen peroxide in human urine: implications for antioxidant defense and redox regulation. Biochem Biophys Res Commun. 1999; 262; 605–609.
24. Kunchandy E, Rao MNA. Oxygen radical scavenging activity of curcumin. Int J Pharm. 1990; 58: 237-240.
25. Fontana M, Mosca L, Rosei MA. Interaction of enkephalins with oxyradicals. Biochem Pharmacol. 2001; 61: 253–257.
26. Denizot F, Lang R. Rapid colorimetric assay for cell growth and survival: modifications to the Tetrazolium dye procedure giving improved sensitivity and reliability. J Immunol Methods. 1986; 89: 271–277.
27. Vignesh V, Felix Anbarasi K, Karthikeyeni S, Sathiyanarayanan G, Subramanian P, Thirumurugan R. A superficial phyto-assisted synthesis of silver nanoparticles and their assessment on hematological and biochemical parameters in *Labeo rohita* (Hamilton 1822). Colloids Surf A. 2013; 439: 184–192.
28. Shanker K, Krishna Mohan G, Mayasa V, Pravallika L. Antihyperglycemic and anti-hyperlipidemic effect of biologically synthesized silver nanoparticles and *G sylvestre* extract on streptozotocin induced diabetic rats-an in vivo approach. Mater Lett. 2017; 195: 240–244.
29. Kassem MES, Ibrahim F, Hussein SR, El-Sharawy R, El-Ansari MA, Hassanane MM, Booles HF. Myricitrin and bioactive extract of *Albizia amara* Leaves: DNA protection and modulation of fertility and antioxidant-related genes expression. Pharm Biol. 2016; 54: 2404–2409.
30. Das D, Ghosh R, Mandal P. Biogenic synthesis of silver nanoparticles using S1 genotype of *Morus alba* leaf extract: characterization antimicrobial and antioxidant potential assessment. SN Appl Sci. 2019; 1: 498.
31. Bhakya S, Muthukrishnan S, Sukumaran M, Muthukumar M. Biogenic synthesis of silver nanoparticles and their antioxidant and antibacterial activity. Appl Nanosci. 2016; 6: 755–766.
32. Mates JM, Sanchez-Jimenez FM. Role of reactive oxygen species in apoptosis: implications for cancer therapy. Int J Biochem Cell Biol. 2000; 32: 157–170.
33. Ramalho SD, Bernades A, Demetrius G, Noda-Perez C, Vieira PC, Dos Santos CY, Da Silva JA, De Moraes MO, Mousinho KC. Synthetic chalcone derivatives as inhibitors of cathepsins K and B and their cytotoxic evaluation. Chem Biodivers. 2013; 10: 1999–2006.
34. Vivek R, Thangam R, Muthuchelian K, Gunasekaran P, Kaveri K, Kannan S. Green biosynthesis of silver nanoparticles from *Annona squamosa* leaf extract and it's in vitro cytotoxic effect on MCF-7 cells. Process Biochem. 2012; 47: 2405–2410.
35. Mousavi-Khattat M, Keyhanfar M, Razmjou A. A comparative study of stability antioxidant DNA cleavage and antibacterial activities of green and chemically synthesized silver nanoparticles. Artif Cells Nanomed Biotechnol. 2018; 46: 1022-1031.
36. Amin KM, Taha AM, George RF, Mohamed NM, Elsenduny FF. Synthesis antitumor activity evaluation and DNA-binding study of coumarin-based agents. Archiv Der Pharmazie. 2018; 351: 1700199.

Cite this article: Kar P, Oriola AO, Singh M, Oyedeji AO. Myricitrin-Mediated Biogenic Silver Nanoparticle Synthesis, Characterization, and its Antioxidant, Anticancer, and DNA Cleavage Activities. Pharmacogn J. 2025;17(2): 121-128.